Bimodality in super-oxidizing and -reducing behavior of Indigo: Dramatic expansion of the redox window by two-electron redox processes

Monojit Roy,[1] Shyamali Maji,[1] Vikramjeet Singh,[1] Dhananjay Dey,[1] Debashis Adhikari[1]*

[1]Department of Chemical Sciences, IISER Mohali, Mohali, Punjab-140306, India. *e-mail: adhikari@iisermohali.ac.in

Indigo is an extremely popular molecule in dye industry, however, its use in photochemical transformations is surprisingly scarce. This report explores its photocatalytic activity over an unusually wide excited-state redox window. To illustrate further, the dye molecule exhibits bimodality and proves itself as a simultaneous super-reductant and -oxidant, spanning a massive redox window of 5.98 V. This extreme bimodal behavior in indigo originates from the viability of two electron redox processes on the parent architecture. In comparison, major popular photocatalysts (PC) usually can accept or donate only one electron, limiting the span of its bimodal redox window significantly. In the presence of KO^{t}Bu and white light irradiation, indigo is converted to its tetraanionic form, Ind^{4-} which displays its super-reducing power to an extent of -3.6 V vs SCE. Such an in situ-generated species has been separately synthesized and the reductive prowess of the PC has been examined for a wide array of reactions which starts with a reductive cleavage of the C-Cl bonds. On the contrary, the super-oxidant behavior of indigo has been explored in the presence of a mild oxidant and blue light irradiation, generating dehydroindigo. The strong oxidizing capability of the PC has been utilized for ipso-substitution of aryl fluorides with a series of nitrogen-based nucleophile.

Visible light photoredox catalysis has likely seen a renaissance in recent times and became a powerful tool for solving challenging chemical transformations that are sometimes even impossible to achieve by thermal pathways.[1–5] The utility of these catalysis processes further lies in the selective activation of specific functional groups by appropriate photon energy, keeping other vulnerable groups intact during those transformations. Earlier developments in photocatalysis heavily utilized ruthenium,[6,7] iridium,[8–10] platinum-based[11,12] catalysts while there is a clear shift in momentum to discover more organic photocatalysts as they could be more sustainable and environmentally benign. A broad interest in developing new organic photocatalysts (PC) or unraveling a new facet of existing photoactive molecules propel the recent photochemical research. Typically, a PC absorbs photon and reaches its electronic excited state which facilitates either energy or electron transfer to different substrate molecules. Different strategies have also been further devised to harness the reducing or oxidizing power of a photocatalyst at its excited state.[13–18] Tandem electro-photochemical approach,[19–21] sensitization-enhanced electron transfer (SenI-ET),[15,22] consecutive photoexcited electron transfer (con-PET) are few of the popular techniques in this direction.[3,5,16,23–26] In the context of excited-state reducing/oxidizing power of a PC molecule, its ability to operate in both directions is an important attribute to the PC (Figure 1a).[27] Such accessibility of bimodal operation ensures that each oxidative or reductive transformation does not require a tailor-made PC. Some of the widely-used transition metal-based photocatalysts exhibit bimodality, however, over a rather narrow range. For example, $[Ru(bpy)_3]^{2+}$ displays the excited state oxidation and reduction potentials at -0.81 V and + 0.77 V (vs SCE), respectively,[27,28] spanning an excited state redox window of 1.58 eV. Similarly, *fac*-Ir(ppy)$_3$ photocatalyst displays the same potentials at -1.73 V and +0.31 V, respectively, covering a potential range of 2.04 eV (Figure 1b).[27,28] Organic photocatalysts, often owing to their high excitation energy ($E_{o,o}$) affords a sizable redox window; for example 4CzIPN spans a window of 2.61 eV. However, the excited state oxidation potential for the aforementioned PC, -1.18 V is barely adequate to break a difficult-to-reduce aryl chloride bond (E_{red} = -2.8 V vs SCE). By the same token, the excited state reduction potential of the same catalyst, +1.43 V is nowhere close to oxidize the reluctant arenes, since such substrate molecules demand an oxidation potential of + 2 V or even higher.[29] Henceforth, a single PC molecule that can afford a very large excited-state redox window, eliciting the simultaneous super-reductant and super-oxidant trait is virtually unknown.

In a closer scrutiny, the bottleneck directly hints to the operational mode of these PC. Almost invariably, the PC at its excited state releases one electron to reductively cleave a target bond, or it accepts an electron to conduct oxidative transformation to the substrate molecule. So, the span of its excited state potential encompassing both oxidative and reductive end is limited by single electron redox event. This limitation primarily stems from the inherent nature of the PC, where two electron redox events are not accessible. Intuitively, if a PC affords two electron redox processes in both direction without any detrimental bond cleavage, there is a strong possibility that it will virtually double its operational redox window. To illustrate, a PC molecule can act simultaneously as both super-reductant and super-oxidant once it can manage two-electron redox transformations onto it. We identify a popular dye indigo that possesses a cross conjugated *p*-quinone and a *p*-phenylene

diamine-type architecture.[30,31] We posit such redox motifs will allow to perform two electron oxidation and two electron reduction discretely so that the excited state window can reach a massively large value. Herein it is further demonstrated that simple in situ chemical modification of indigo by an extremely mild reductant and a mild oxidant can prepare the highly reducing and oxidizing states so that their super-redox trait can be harnessed over an unusually wide potential window of 5.98 eV (Figure 1a).

Indigo's prolific use as dying element to cloths, fabrics are age old.[32-34] The deep blue color and immense photostability of the indigo under sunlight are perhaps the reason behind its enormous popularity as a dying agent. Its tremendous photostability even sparked research interest to find means to decompose such molecule in the presence of a catalyst. Surprisingly, such a robust photocatalyst has not been examined widely for steering photochemical reactions. Parent indigo molecule, **$IndH_2$** strongly absorbs in the visible region (620 nm) and result in dark blue color appearance (Figure 2a). To augment the reductive prowess of indigo, we treated **$IndH_2$** with a mild reductant KO^{t}Bu and was able to reduce it in full under white light excitation by a LED lamp. Our primary plan is motivated by con-PET mode, so that one-electron-reduced **$IndH_2$** is further photoexcited and becomes strongly reducing.[3,16] However, higher equivalent of KO^{t}Bu completely deprotonated the starting species, parallel to its double reduction, generating **Ind^{4-}**.[35] The color of the putative species dramatically changes to red-violet from the starting blue color of parent **$IndH_2$** (see supplementary information for details, Section 4.2). This **Ind^{4-}** species is extremely reducing in character and reductively cleave a very demanding aryl chloride as well as aryl fluoride bond (*vide infra*).[19] The putative tetraanion intermediate is distinctly different from doubly-reduced *leuco* indigo, which is widely used in the dye industry to make the indigo water soluble.[36] The present active catalyst **Ind^{4-}** is doubly deprotonated in tandem with two-electron reduction. To ascertain that double deprotonation of **$IndH_2$** is required on top of two-electron reduction, we performed a control reaction (see supplementary information for details, Section 4.4.c). We used a strong reductant, metallic sodium (2 equiv.) to completely reduce **$IndH_2$** and authenticated the *leuco* form by the presence of the N-H proton resonating at 10.5 ppm. Such a doubly reduced, yet protonated *leuco*-indigo species was employed to break a recalcitrant aryl chloride bond. Notably, the leuco form was unable to perform such challenging reduction, strongly suggesting photoexcitation of **Ind^{4-}** stage is necessary to elicit its super-reducing behavior. The **Ind^{4-}** form is sensitive to oxygen, however the molecule can remain stable for weeks in an inert atmosphere of a glove box. To gauge the extreme reducing power of this form, we at first measured its ground state oxidation potential by cyclic voltammetry. In electrochemical time scale it displays an irreversible wave at a peak potential of -1.2 V vs SCE (see supplementary information for details, Section 4.3.a). The tetraanionic molecule shows a broad absorption from 400-550 nm, with a maximum around 478 nm (Figure 2b). When excited at 478 nm, **Ind^{4-}** fluoresces at 540 nm. The excitation energy $E_{o,o}$ is calculated to be 2.4 eV from the intersecting point of its absorption and emission spectra. Using the Rehm-Weller equation, the excited state potential can be estimated as E* = -1.2-2.4 V = -3.6 V vs SCE (see supplementary information for details, Section 5).[37] Since we are accounting for the peak potential of the anodic wave, rather a truly reversible potential, we may take this potential as the upper limit of its reducing power. Nevertheless, such a large negative redox potential justifies completely its super-reducing behavior of the in situ-generated **Ind^{4-}** upon visible light excitation condition. To investigate further the excited state electron transfer from the putative species to aryl chlorides, a Stern-Volmer quenching experiment was conducted. Along this direction, a gradual increase in chlorobenzamide concentration resulted in sequential decrease of fluorescence intensity of **Ind^{4-}** at 540 nm. Once the ratio of fluorescence intensities (in the absence and in the presence of quencher) was plotted with increasing chlorobenzamide substrate concentration, a clear straight line with an K_{SV} value of 785 M^{-1} was derived (see supplementary information for details, Figure S12-S13). Apparently, the administered base KO^{t}Bu plays a dual role of doubly reducing the indigo, and simultaneously doubly deprotonating to generate the most reactive **Ind^{4-}** form. To examine the fate of this reductive catalyst, we prepared the **Ind^{4-}** species in situ by the addition of 4.5 equiv of KO^{t}Bu to a DMSO solution of **$IndH_2$** under visible light and added one equivalent of substrate chlorobenzene. The radical anion, **Ind^{3-}** was generated instantaneously upon visible light excitation that was clearly detected by X-band EPR spectroscopy at room temperature. A broad signal at g = 1.92 emerges without any discernible hyperfine couplings from the nitrogen at room temperature. However, the broad nature of the signal likely testifies for the delocalized nature of the radical generated at the indigo backbone upon an electron transfer from the PC (see supplementary information for details, Section 7). We will be showing through a plethora of reactivity studies that this **Ind^{4-}** promptly transfers electron via photoinduced electron transfer (PET) pathway to reductively demanding substrate molecules.

We reiterate that **Ind^{4-}** is the in situ-generated active species that elicit such a strong reducing power. To nullify that simple di-deprotonated indigo **Ind^{2-}** is not capable of directing reductive cleavage under such a demanding potential, we prepared the latter by deprotonating both -NH protons of **$IndH_2$** by Cs_2CO_3. It has been proved earlier that Cs_2CO_3 is sufficiently basic to carry out the complete deprotonation.[38] However, this doubly deprotonated form under visible light irradiation converted the test substrate 2-Chloro-*N*,*N*-bis(1-methylethyl)benzamide to isoindolinone in mere 11% yield (Figure 2e). To substantiate our hypothesis further, that double deprotonation is required in parallel to two-electron reduction, we synthesized a N,N'-diphenyl indigo where two N-H protons have been replaced by phenyl groups (see supplementary information for

details, Section 4.4.e).[38,39] Logically, upon photoexcitation, N,N'-diphenyl indigo can only be doubly reduced. In strong agreement with our conjecture, such a modified indigo molecule was not highly reducing. Taking *p*-chloro anisole as a model substrate, a cross-coupling reaction was performed in benzene to obtain the C-C cross-coupled product in a poor 25% yield (see supplementary information for details, Section 4.4.f). This lack of extreme reductive power in $\mathbf{Ind^{-2}}$ is also in alignment with CV data. The electrochemical analysis proves that $\mathbf{Ind^{-4}}$ is approximately 1 V more reducing in its ground state than $\mathbf{Ind^{-2}}$ (see supplementary information for details, Section 4.3.b). Taken together, all these experiments strongly suggest that double deprotonation and simultaneous two-electron reduction are the requisite to prepare the super-reducing species. Very importantly, all these processes happen in the presence of KO^{t}Bu under visible light.

After exploring the reductive end of the indigo molecule, we set out to explore its oxidative prowess. We anticipate, the presence of *p*-phenylene diamine architecture will help to reach dehydroindigo (**Ind**), upon $2e^-/2H^+$ removal from parent $\mathbf{IndH_2}$.[30] The **Ind** form is the most oxidized state of indigo, and will likely be a super-oxidizing species upon photoexcitation. With this goal we identified potassium peroxodisulfate to be the desired oxidant that oxidizes $\mathbf{IndH_2}$ completely. This oxidation also happens under visible light excitation, which cleanly generates the dark brown solid **Ind** in quantitative yield. The chosen oxidant works very efficiently given the hydrogen atom abstraction ability of $SO_4^{\bullet-}$, generated from $S_2O_8^{2-}$ promoting oxidation . The importance of visible light initiation was investigated further and it was proved that the oxidation did not proceed at all under dark condition. The fully oxidized **Ind** is a very much stable molecule which can be purified by column chromatographic separation to isolate a dark brown granular solid. The nature of the isolated molecule was confirmed by its absorption, emission, electrochemical behavior and high-resolution ESI-MS spectrometry. The spectroscopic signature of the molecule corroborates well with prior literature report.[30] The molecule in DMSO solution absorbs at 397 nm which is compatible with the observed color for the molecule (Figure 3a). The ground state reduction of the molecule occurs at -0.43 V vs SCE, which can be translated to its excited state reduction potential as +2.38 V vs SCE (see supplementary information for details, Section 5). This value further promises that in situ-generated **Ind** will be a super-oxidant and will activate many reluctant substrates in an oxidative fashion.

To evaluate the synthetic potential of indigo to reductively cleave aryl halide bonds, we started our foray with an array of α-chloro amide substrates.[40,41] The standard reaction conditions was optimized to involve 3 mol% indigo loading in the presence of 3 equivalent of base KO^{t}Bu. The reaction mixture was irradiated with a white LED (see supplementary information for optimization details, Section 2.1). Under this condition, the α-chloro amide **1** afforded the isoindolinone in 93% yield. Interestingly, it was observed that the reactions finished in 4 h, attributable to the highly reactive nature of the super-reductant $\mathbf{Ind^{4-}}$. Substrates with N,N'-ethyl, -isopropyl groups selectively went for 1,5-HAT from the isopropyl motif to result isoindolinone **2** in 87% , (Figure 4) yield. Varying the substitutions at the amide nitrogen to methyl and benzyl were well tolerated and the reaction smoothly converted these substrates to the respective isoindolinones **3** and **4** in 86-89% yields. A variety of substitutions at the phenyl ring including -Me at the *meta* or *para* position survived well the reaction condition to furnish isoindolinones (**5-6**, Figure 4) in 77-88% yields. Heterocyclic ring pyridine also afforded the final isoindolinone product **7** in 78% yield. Furthermore, a set of sophisticated isoindolinones (**8-9**, Figure 4) were also prepared by this methodology in 78-86% yields. Spirocyclic isoindolinone can also be synthesized under this method as isoindolinone **10** was prepared in high, 87% yield. After that the starting substrate was varied to N-alkylated α-chloro anilides. The chosen anilide responded equally well under the optimized reaction condition to afford the oxindolinone **11** in 84% yields. Electron donating methoxy, methyl groups in the chloro anilide furnished products **12-14** in 71-78% yields. On the other hand, strongly electron withdrawing functional groups such as trifluoromethyl, nitro, cyano groups responded well to the reaction conditions to furnish **15-17** in 68-88% yields. Furthermore, a spirocyclic oxindolinone **18** was synthesized under this developed methodology in 81% yield. Next, N-benzyl acetamide was examined, which smoothly converted to the N-benzyl oxindole **19** product in 68% yield. Similarly, α-halo benzamides **20** assembled the corresponding phenanthridinone products in high yields (81%). Interestingly, phenanthridione **21,** a known precursor of antitumor agent was synthesized in 79% yield. Finally a bioactive alkaloid phenaglydon, **22** was assembled in 83% yield, starting from an aryl bromo precursor molecule.[42]

After that, we exploited the power of indigo as a strongly reductive photocatalyst in a series of C-C, C-B and C-P bond formation reactions.[3,19] For this set of reactions, unsubstituted aryl chlorides were chosen as substrate, which are very difficult-to-break via single electron transfer pathway.[43] In this manner these substrates can truly gauge the reductive capability of the PC, as unsubstituted or electron rich aryl chlorides require a potential of *ca* -2.9 V vs SCE to promote reductive cleavage.[44] Following this methodology, a series of aryl chloride molecules were utilized as an aryl radical precursor and cross-coupled with a different heteroarenes such as *N*-methyl pyrrole, thiophenes or furans. The C-C cross-coupling products (**23-26**, Figure 5) were isolated in 55-64% yields. The reaction was performed in a relatively redox inert solvent DMSO, however the moderate yield of the cross-coupled product may originate from super-reducing $\mathbf{Ind^{4-}}$, which makes the DMSO a vulnerable molecule towards reduction. Furthermore, α-naphthyl chloride was reductively cleaved to generate the corresponding naphthyl radical which was

coupled to *N*-methyl pyrrole to result **27** in 59% yield. Similarly, the *p*-trifluoromethyl chlorobenzene was examined with furan to synthesize **28** in 65% yield. The *m*-methyl, *p*-methoxy, *p*-cyano, 3,5-dimethyl chlorobenzene were reductively cleaved and cross-coupled to thiophene to furnish products **29-32** in 57-71% yields. Naphthyl chloride and 5-methoxy naphthyl chlorides were similarly cross-coupled to thiophenes to provide **32-33** in 58-64% yields. Analogously, a photo-Arbuzov reaction was attempted with aryl chloride to prepare aryl phosphonates, which resulted in the preparation of **35** in 52% yield.[45] Furthermore, a series a borylation reaction was investigated starting from aryl chloride substrate in the presence of pinacol borane. Gratifyingly, five different aryl boronates **36-40** were synthesized in 49-64% yields following our developed protocol. A series of C-C cross-coupled products were assembled using benzene as the reaction partner. Aryl chlorides with electron withdrawing trifluoromethyl, cyano groups resulted in cross-coupled product **41-42** with benzene in 78-81% yields. The electron donating aryl chloride such as p-methoxy aryl chloride afforded moderate, 58% yield of the product **43**. The same product can also be attempted from even more challenging substrate like aryl fluoride, however the product forms in poor yield.[4,43] We further attribute the lower yield to competitive reduction of DMSO at such a demanding potential, at which the **Ind**$^{4-}$ is capable of delivering an electron towards reductive cleavage reaction. Different naphthyl chloride/bromides were successfully cross-coupled to furnish **50, 51, 53** in 62-81% yields. Such cross-coupling reactions can be stretched to polycyclic rings effectively. Accordingly, 1,4- and 1,3- dibromobenzene can be easily converted to triphenyl **54** and **56** in 54-57% yields. Encouragingly, several heterocyclic aryl halides such as pyridyl or thiophenyl chlorides were tested further, which can furnish the desirable C-C cross-coupled products **57-60** in moderate to good yield.

After successfully expanding the substrate scope at the reductive end (**Ind**$^{4-}$), we sought to explore the oxidative prowess of the catalyst (**Ind**). Along this goal, we chose a nucleophilic aromatic substitution reaction. If oxidatively demanding fluoroarenes can be oxidized, a nucleophile can attack and through further electron transfer may furnish the C-N coupled product. When Indigo in presence of 2 equiv. of $K_2S_2O_8$ was used under photoexcitation, *p*-methoxy fluoroarene was conveniently converted to the C-N coupled product **61** in 72% yield (see supplementary information for optimization details, Section 2.2). A variety of nucleophiles including triazole, benzimidazole and benzotriazole were examined for the S_NAr reaction, successfully affording the desired products **62, 63, 65** in 24-60% yields (Figure 3). Furthermore, the *ortho*-substituted electron-rich systems readily underwent S_NAr C-F substitution with 4-iodopyrazole and 4-carboxylatepyrazole to afford the products **64** and **66** in 60-67% yields. Methyl substituted fluorobenzene also showed promising reactivity under this protocol when the nucleophile was selected to 4-carboxylate pyrazole resulting into the desired products **67-68** in 59-62% yields. Finally, the nucleophile was changed to 2H-1,2,3-triazole and it was reacted with 3,4-dimethoxyfluorobenzene to synthesize **69** in 50% yield.

In conclusion, we showcase that indigo, an unexplored photocatalyst possesses tremendous potential in directing a plethora of photochemical transformations. The presence of a quinone-type and aminoquinol-type cross-conjugated motif in indigo gives access to two-electron reduction, as well as two-electron oxidation. Furthermore, the presence of two deprotonable N-H groups affords double deprotonation to prepare a super-reductant motif. This architectural pattern facilitates affording simultaneous super-reductant and -oxidant behavior over a colossal redox window of 5.98 V. Compared to this value, a large number of photocatalysts are limited to access a potential window of ~ 3 V, likely stems from their ability to be oxidized or reduced by single electron only. We believe this study is a great entry point for utilizing indigo as a photocatalyst, and to show what design principle can elicit simultaneously strong reductive and oxidative chemistry from a single molecule.

References-

1. Chan, A. Y. *et al.* Exploiting the Marcus inverted region for first-row transition metal–based photoredox catalysis. *Science.* **382**, 191–197 (2023).
2. Tian, L., Till, N. A., Kudisch, B., MacMillan, D. W. C. & Scholes, G. D. Transient Absorption Spectroscopy Offers Mechanistic Insights for an Iridium/Nickel-Catalyzed C–O Coupling. *J. Am. Chem. Soc.* **142**, 4555–4559 (2020).
3. Xu, J. *et al.* Unveiling Extreme Photoreduction Potentials of Donor–Acceptor Cyanoarenes to Access Aryl Radicals from Aryl Chlorides. *J. Am. Chem. Soc.* **143**, 13266–13273 (2021).
4. Halder, S., Mandal, S., Kundu, A., Mandal, B. & Adhikari, D. Super-Reducing Behavior of Benzo[b]phenothiazine Anion Under Visible-Light Photoredox Condition. *J. Am. Chem. Soc.* **145**, 22403–22412 (2023).
5. Cole, J. P. *et al.* Organocatalyzed Birch Reduction Driven by Visible Light. *J. Am. Chem. Soc.* **142**, 13573–13581 (2020).
6. Narayanam, J. M. R., Tucker, J. W. & Stephenson, C. R. J. Electron-Transfer Photoredox Catalysis: Development of a Tin-Free Reductive Dehalogenation Reaction. *J. Am. Chem. Soc.* **131**, 8756–8757 (2009).
7. Maji, T., Karmakar, A. & Reiser, O. Visible-Light Photoredox Catalysis: Dehalogenation of Vicinal Dibromo-, α-Halo-, and α,α-Dibromocarbonyl Compounds. *J. Org. Chem.* **76**, 736–739 (2011).
8. Li, C.-G., Xu, G.-Q. & Xu, P.-F. Synthesis of Fused Pyran Derivatives via Visible-Light-Induced Cascade Cyclization of 1,7-Enynes with Acyl Chlorides. *Org. Lett.* **19**, 512–515 (2017).
9. Föll, T., Rehbein, J. & Reiser, O. $Ir(ppy)_3$ -

Catalyzed, Visible-Light-Mediated Reaction of α-Chloro Cinnamates with Enol Acetates: An Apparent Halogen Paradox. *Org. Lett.* **20**, 5794–5798 (2018).
10. Jiang, M., Li, H., Yang, H. & Fu, H. Room-Temperature Arylation of Thiols: Breakthrough with Aryl Chlorides. *Angew. Chem., Int. Ed.* **56**, 874–879 (2017).
11. Maiti, S. *et al.* Light-induced Pd catalyst enables $C(sp^2)$–$C(sp^2)$ cross-electrophile coupling bypassing the demand for transmetalation. *Nat. Catal.* **7**, 285–294 (2024).
12. Zhou, W. *et al.* Visible-Light-Driven Palladium-Catalyzed Radical Alkylation of C−H Bonds with Unactivated Alkyl Bromides. *Angew. Chem., Int. Ed.* **56**, 15683–15687 (2017).
13. Murray, P. R. D. *et al.* Photochemical and Electrochemical Applications of Proton-Coupled Electron Transfer in Organic Synthesis. *Chem. Rev.* **122**, 2017–2291 (2022).
14. MacKenzie, I. A. *et al.* Discovery and characterization of an acridine radical photoreductant. *Nature* **580**, 76–80 (2020).
15. Ghosh, I., Shaikh, R. S. & König, B. Sensitization-Initiated Electron Transfer for Photoredox Catalysis. *Angew. Chem., Int. Ed.* **56**, 8544–8549 (2017).
16. Ghosh, I., Ghosh, T., Bardagi, J. I. & König, B. Reduction of aryl halides by consecutive visible light-induced electron transfer processes. *Science.* **346**, 725–728 (2014).
17. Bortolato, T. *et al.* The Rational Design of Reducing Organophotoredox Catalysts Unlocks Proton-Coupled Electron-Transfer and Atom Transfer Radical Polymerization Mechanisms. *J. Am. Chem. Soc.* **145**, 1835–1846 (2023).
18. Jin, S. *et al*. Visible Light-Induced Borylation of C–O, C–N, and C–X Bonds. *J. Am. Chem. Soc.* **142**, 1603–1613 (2020).
19. Cowper, N. G. W., Chernowsky, C. P., Williams, O. P. & Wickens, Z. K. Potent Reductants via Electron-Primed Photoredox Catalysis: Unlocking Aryl Chlorides for Radical Coupling. *J. Am. Chem. Soc.* **142**, 2093–2099 (2020).
20. Kim, H., Kim, H., Lambert, T. H. & Lin, S. Reductive Electrophotocatalysis: Merging Electricity and Light To Achieve Extreme Reduction Potentials. *J. Am. Chem. Soc.* **142**, 2087–2092 (2020).
21. Chernowsky, C. P., Chmiel, A. F. & Wickens, Z. K. Electrochemical Activation of Diverse Conventional Photoredox Catalysts Induces Potent Photoreductant Activity. *Angew. Chem., Int. Ed.* **60**, 21418–21425 (2021).
22. Ghosh, I., Bardagi, J. I. & König, B. Reply to "Photoredox Catalysis: The Need to Elucidate the Photochemical Mechanism". *Angew. Chem., Int. Ed.* **56**, 12822–12824 (2017).
23. Brandl, F., Bergwinkl, S., Allacher, C. & Dick, B. Consecutive Photoinduced Electron Transfer (conPET): The Mechanism of the Photocatalyst Rhodamine 6G. *Chem. Eur. J.* **26**, 7946–7954 (2020).
24. Fang, Y., Liu, T., Chen, L. & Chao, D. Exploiting consecutive photoinduced electron transfer (ConPET) in CO_2 photoreduction. *Chem. Commun.* **58**, 7972–7975 (2022).
25. Caby, S., Bouchet, L. M., Argüello, J. E., Rossi, R. A. & Bardagi, J. I. Excitation of Radical Anions of Naphthalene Diimides in Consecutive- and Electro-Photocatalysis. *ChemCatChem* **13**, 3001–3009 (2021).
26. Ghosh, I. & König, B. Chromoselective Photocatalysis: Controlled Bond Activation through Light-Color Regulation of Redox Potentials. *Angew. Chem., Int. Ed.* **55**, 7676–7679 (2016).
27. Speckmeier, E., Fischer, T. G. & Zeitler, K. A Toolbox Approach To Construct Broadly Applicable Metal-Free Catalysts for Photoredox Chemistry: Deliberate Tuning of Redox Potentials and Importance of Halogens in Donor–Acceptor Cyanoarenes. *J. Am. Chem. Soc.* **140**, 15353–15365 (2018).
28. Prier, C. K., Rankic, D. A. & MacMillan, D. W. C. Visible Light Photoredox Catalysis with Transition Metal Complexes: Applications in Organic Synthesis. *Chem. Rev.* **113**, 5322–5363 (2013).
29. Huang, H. & Lambert, T. H. Electrophotocatalytic S N Ar Reactions of Unactivated Aryl Fluorides at Ambient Temperature and Without Base. *Angew. Chem., Int. Ed.* **59**, 658–662 (2020).
30. Rondão, R., Seixas de Melo, J. S., Bonifácio, V. D. B. & Melo, M. J. Dehydroindigo, the Forgotten Indigo and Its Contribution to the Color of Maya Blue. *J. Phys. Chem. A* **114**, 1699–1708 (2010).
31. Seixas de Melo, J., Moura, A. P. & Melo, M. J. Photophysical and Spectroscopic Studies of Indigo Derivatives in Their Keto and Leuco Forms. *J. Phys. Chem. A* **108**, 6975–6981 (2004).
32. Novotná, P., Boon, J. J., van der Horst, J. & Pacáková, V. Photoegradation of indigo in dichloromethane solution. *Color. Technol.* **119**, 121–127 (2003).
33. Clark, R. J. H., Cooksey, C. J. & Daniels, Marcus A M Withnall, R. Indigo, woad, and Tyrian Purple : important vat dyes from antiquity to the present. *Endeavour* **17**, 191–199 (1993).
34. Padden, A. N. *et al.* Clostridium used in mediaeval dyeing. *Nature* **396**, 225–226 (1998).
35. Chatterjee, M. *et al.* A structurally characterised redox pair involving an indigo radical: indigo based redox activity in complexes with one or two $[Ru(bpy)_2]$ fragments. *Dalton Trans.* **46**, 5091–5102 (2017).
36. Sala, M. & Gutiérrez-Bouzán, M. C. Electrochemical Techniques in Textile Processes and Wastewater Treatment. *Int. J. Photoenergy* **2012**, 1–12 (2012).
37. Romero, N. A. & Nicewicz, D. A. Organic Photoredox Catalysis. *Chem. Rev.* **116**, 10075–10166 (2016).
38. Huang, C.-Y. *et al.* N , N ′-Disubstituted Indigos as Readily Available Red-Light Photoswitches with

Tunable Thermal Half-Lives. *J. Am. Chem. Soc.* **139**, 15205–15211 (2017).
39. Huang, C. (Dennis) & Hecht, S. A Blueprint for Transforming Indigos to Photoresponsive Molecular Tools. *Chem. Eur. J.* **29**, (2023).
40. Cybularczyk-Cecotka, M., Predygier, J., Crespi, S., Szczepanik, J. & Giedyk, M. Photocatalysis in Aqueous Micellar Media Enables Divergent C–H Arylation and N -Dealkylation of Benzamides. *ACS Catal.* **12**, 3543–3549 (2022).
41. Wertjes, W. C., Wolfe, L. C., Waller, P. J. & Kalyani, D. Nickel or Phenanthroline Mediated Intramolecular Arylation of sp^3 C–H Bonds Using Aryl Halides. *Org. Lett.* **15**, 5986–5989 (2013).
42. Pimparkar, S. & Jeganmohan, M. Palladium-catalyzed cyclization of benzamides with arynes: application to the synthesis of phenaglydon and N-methylcrinasiadine. *Chem. Commun.* **50**, 12116–12119 (2014).
43. Glaser, F., Larsen, C. B., Kerzig, C. & Wenger, O. S. Aryl dechlorination and defluorination with an organic super-photoreductant. *Photochem. Photobiol. Sci.* **19**, 1035–1041 (2020).
44. Chmiel, A. F., Williams, O. P., Chernowsky, C. P., Yeung, C. S. & Wickens, Z. K. Non-innocent Radical Ion Intermediates in Photoredox Catalysis: Parallel Reduction Modes Enable Coupling of Diverse Aryl Chlorides. *J. Am. Chem. Soc.* **143**, 10882–10889 (2021).
45. Shaikh, R. S., Düsel, S. J. S. & König, B. Visible-Light Photo-Arbuzov Reaction of Aryl Bromides and Trialkyl Phosphites Yielding Aryl Phosphonates. *ACS Catal.* **6**, 8410–8414 (2016).

Acknowledgements

Research reported in this publication was supported by the MHRD-STARS grant (STARS2/2023/0474). Financial support received from PMRF (fellowship to M.R.), CSIR-India (fellowship to S.M.), and CSIR-India (fellowship to V.S.), is gratefully acknowledged.

Author contributions

M.R. and D.A. conceived the concept. All authors designed, performed, and analyzed the experimental data. S.M., V.S. and D.D. explored the substrate scope and performed some mechanistic experiments. D.A. supervised the work. and was also responsible for the fund acquisition. M.R. and D.A. prepared the manuscript, with the input from other authors.

Competing interests: The authors declare no other competing financial interests.

Additional information

Supplementary Information

Reprints and permissions information

Correspondence and requests for materials should be addressed to D.A. (adhikari@iisermohali.ac.in).

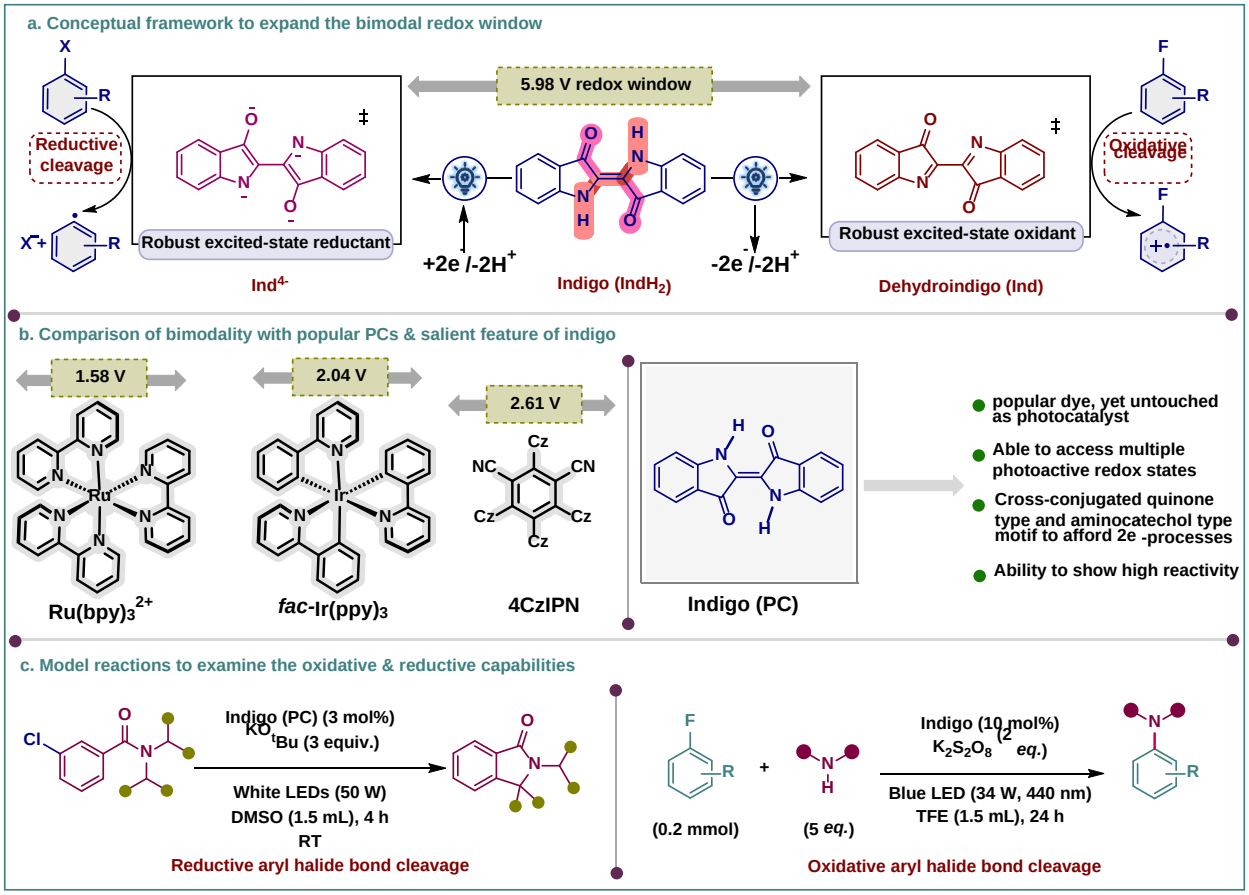

Figure 1 | **Selective C-C and C-N bond formation via Indigo dye as a photocatalyst**. **a**. Conceptual framework to expand the bimodal redox window. **b**. Comparison of bimodality with popular PCs & salient feature of indigo. **c**. Model reactions to examine the oxidative & reductive capabilities.

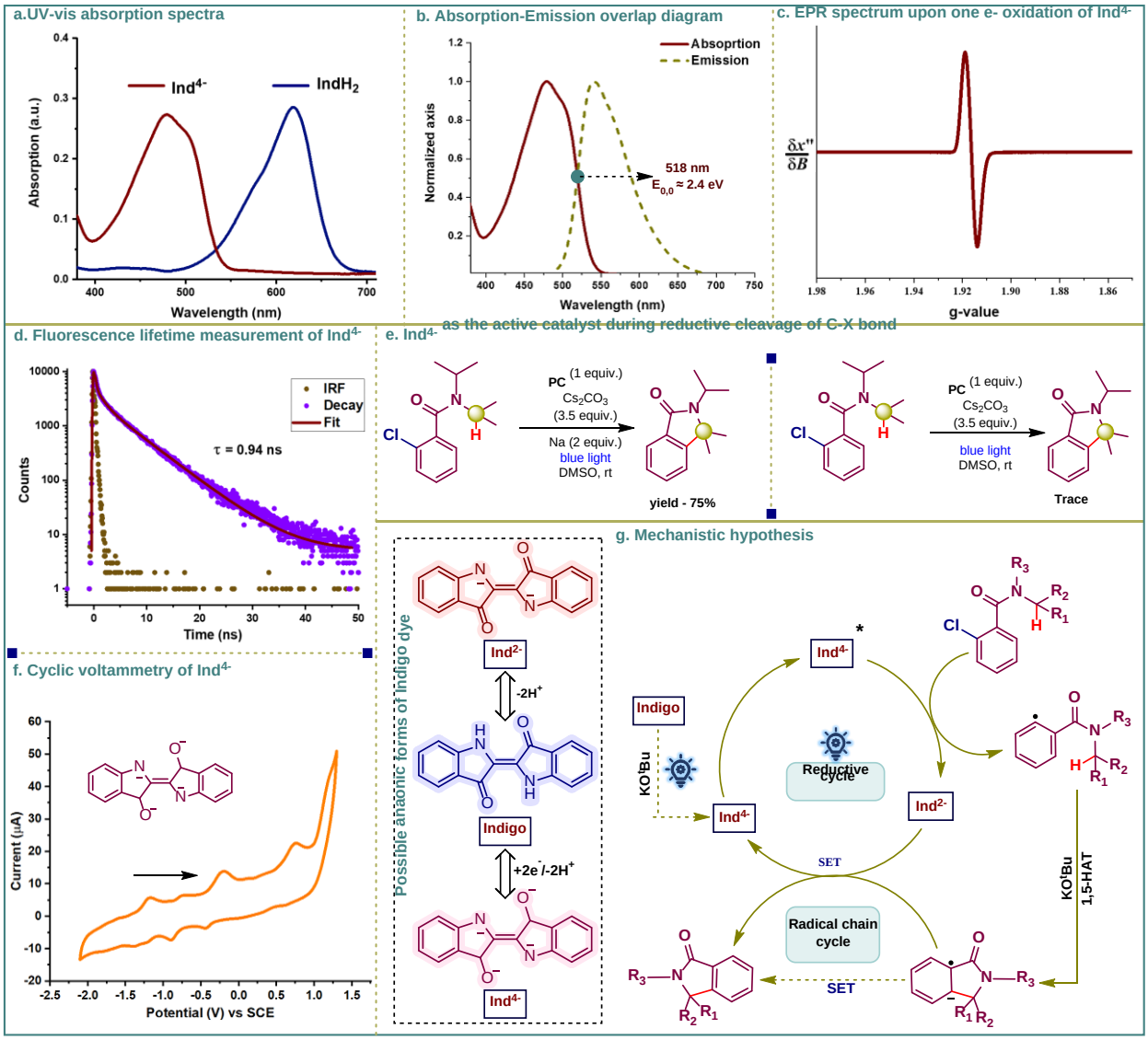

Figure 2 | **Mechanistic studies**. **a**. UV-vis absorption spectra **b**. Absorption-Emission overlap diagram. **c**. EPR spectrum upon one e$^-$ oxidation of Ind^{4-}. **d**. Fluorescence lifetime measurement of **Ind^{4-}**. **e**. Ind^{4-} as the active catalyst during reductive cleavage of C-X bond. **f**. Cyclic voltammetry of Ind^{4-}. **g**. Mechanistic hypothesis.

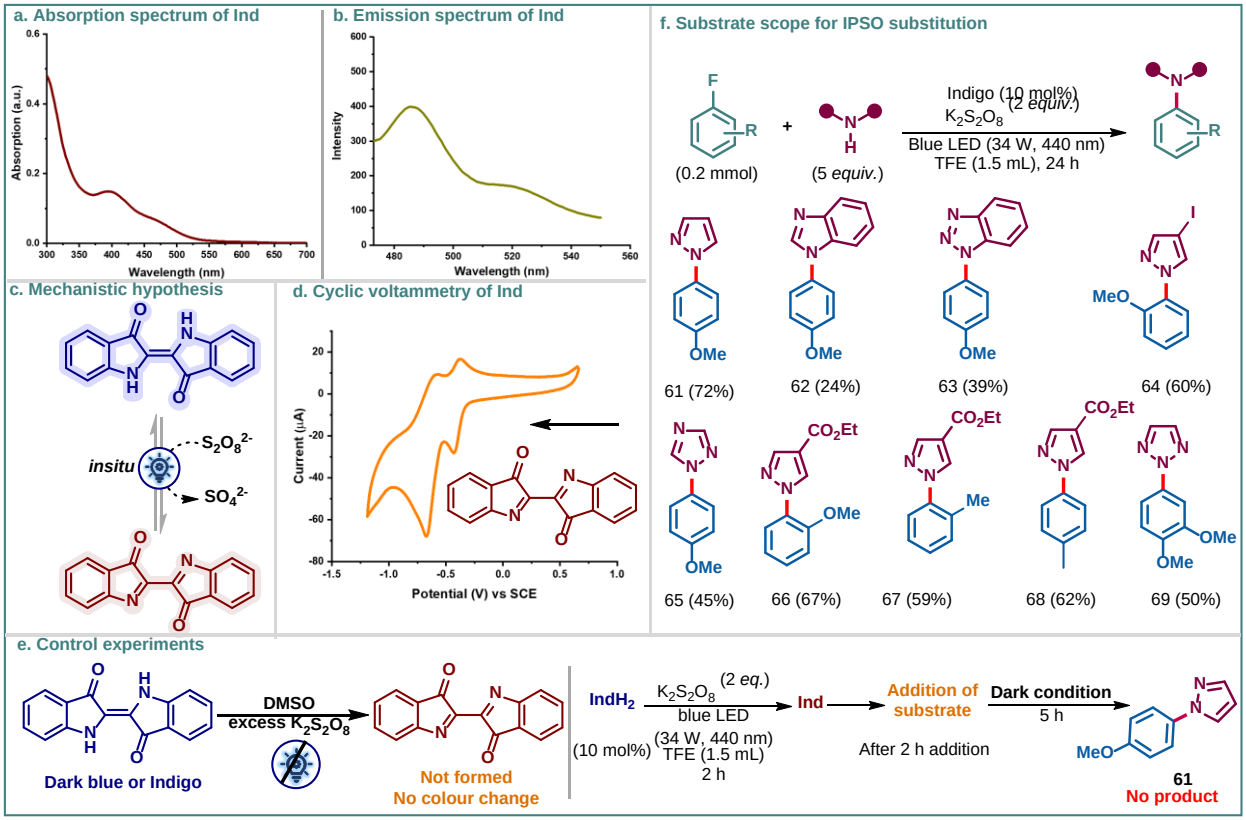

Figure 3 | **Oxidative cleavage. a**. Absorption spectrum of Ind. **b**. Emission spectrum of Ind. **c**. Insitu generation of Ind. **d**. Cyclic voltammetry of Ind. **e**. Control experiments. **f.** Substrate scope for IPSO substitution.

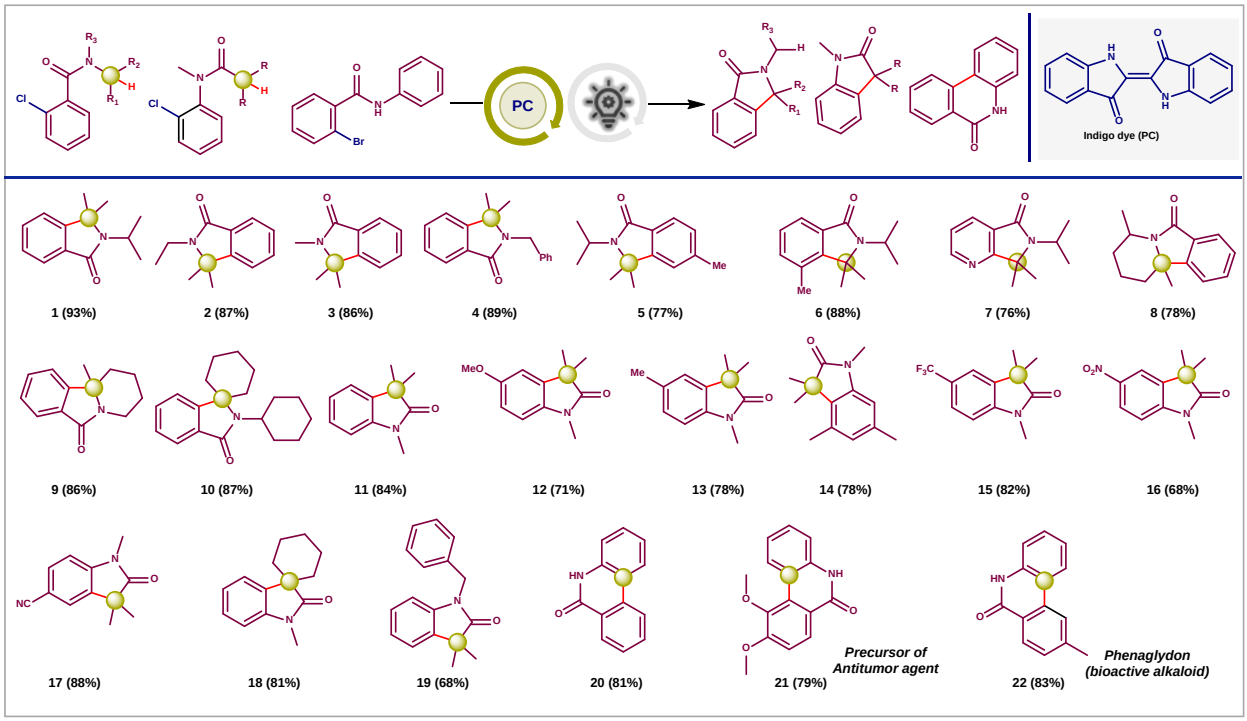

Figure 4 | **Scope of cyclic C-C bond formation reactions.**

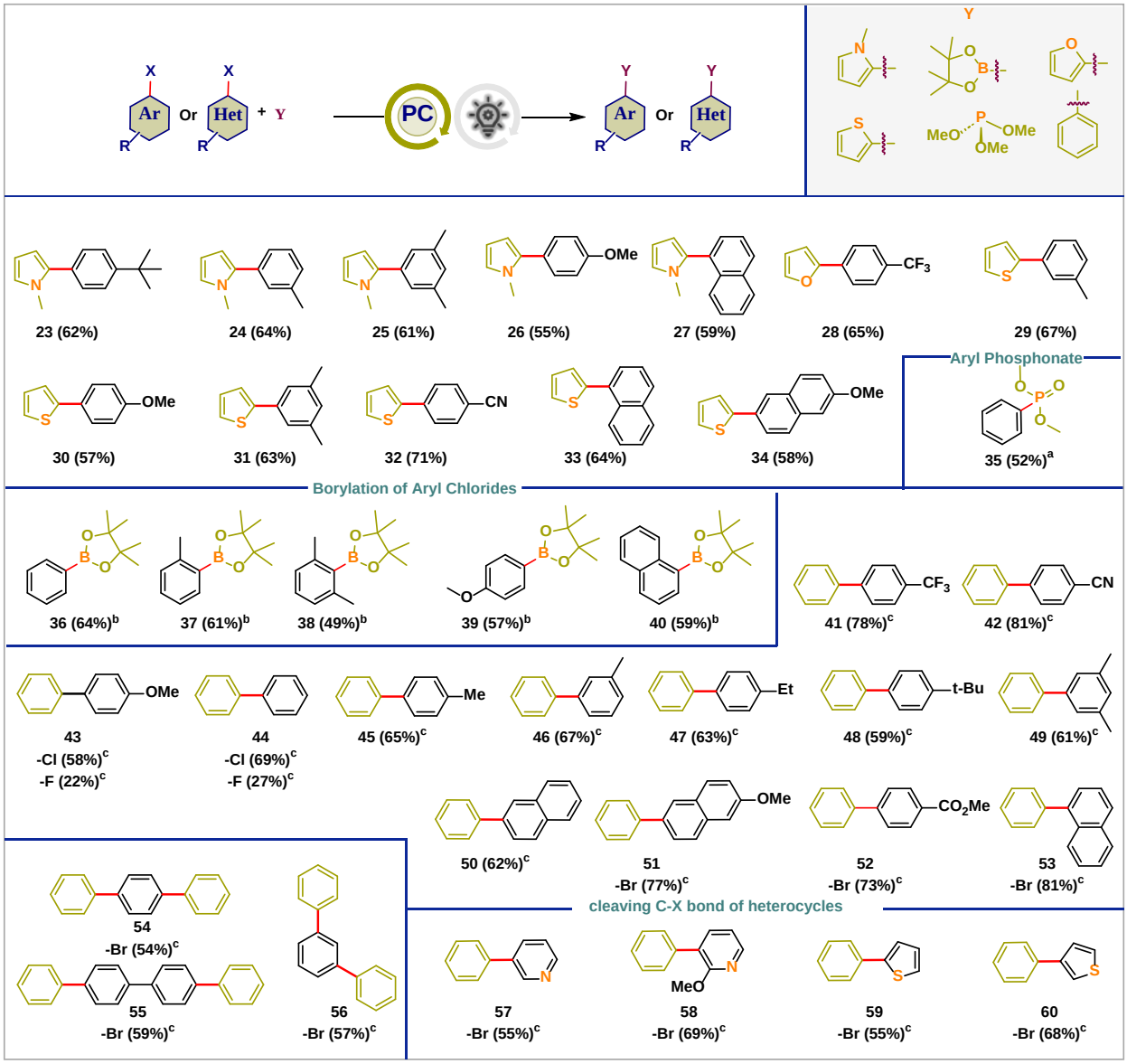

Figure 5 | **Scope of C-C, C-P, C-B, bond formation reactions.** [a]$P(OMe)_3$ (2 mmol), DMSO (1.5 mL). [b]B_2pin_2 (2 mmol), DMSO (1.5 mL). [c]Benzene (2 mL).